Virologica Sinica (2021) 36:608–622
https://doi.org/10.1007/s12250-020-00322-2

www.virosin.org
www.springer.com/12250

RESEARCH ARTICLE

Foot-and-Mouth Disease Virus Inhibits RIP2 Protein Expression to Promote Viral Replication

Huisheng Liu[1] · Qiao Xue[1] · Zixiang Zhu[1] · Fan Yang[1] · Weijun Cao[1] · Xiangtao Liu[1] · Haixue Zheng[1]

Received: 10 July 2020 / Accepted: 17 September 2020 / Published online: 5 January 2021

Abstract

Receptors interaction protein 2 (RIP2) is a specific adaptor molecule in the downstream of NOD2. The role of RIP2 during foot-and-mouth disease virus (FMDV) infection remains unknown. Here, our results showed that RIP2 inhibited FMDV replication and played an important role in the activation of IFN-β and NF-κB signal pathways during FMDV infection. FMDV infection triggered RIP2 transcription, while it reduced the expression of RIP2 protein. Detailed analysis showed that FMDV 2B, 2C, $3C^{pro}$, and L^{pro} proteins were responsible for inducing the reduction of RIP2 protein. $3C^{pro}$ and L^{pro} are viral proteinases that can induce the cleavage or reduction of many host proteins and block host protein synthesis. The carboxyl terminal 105–114 and 135–144 regions of 2B were essential for reduction of RIP2. Our results also showed that the N terminal 1–61 region of 2C were essential for the reduction of RIP2. The 2C-induced reduction of RIP2 was dependent on inducing the reduction of poly(A)-binding protein 1 (PABPC1). The interaction between RIP2 and 2C was observed in the context of viral infection, and the residues 1–61 were required for the interaction. These data clarify novel mechanisms of reduction of RIP2 mediated by FMDV.

Keywords Foot-and-mouth disease virus (FMDV) · Receptors interaction protein 2 (RIP2) · PABPC1 · 2C · Immune evasion

Introduction

Foot-and-mouth disease virus (FMDV), an *Aphthovirus* within the viral family *Picornaviridae*, is a single-stranded positive-sense RNA virus that causes foot-and-mouth disease (FMD) in domestic and wild cloven-hoofed animals worldwide (Belsham 1993; Grubman and Baxt 2004). To date, there are seven known serotypes of FMDV including O, A, Asia1, C, SAT1, SAT2, and SAT3. FMDV contains a genome of approximately 8.4 kb molecule, which encodes a single polyprotein that is subsequently cleaved into 12 proteins including L^{pro}, VP1, VP2, VP3, VP4, 2A, 2B, 2C, 3A, 3B, $3C^{pro}$, and $3D^{pol}$ (Li *et al.* 2016).

FMDV 2BC protein is cleaved into 2B and 2C during viral infection and it suppresses protein trafficking from the endoplasmic reticulum (ER) to the Golgi apparatus (Moffat *et al.* 2005, 2007). FMDV 2B, an approximately 17-kDa protein, is involved in the re-arrangement of host cell membranes (Moffat *et al.* 2005). Furthermore, the carboxyl terminal region of 2B is involved in membrane interaction, which plays important roles in virus replication (Moraes *et al.* 2011). Our previous studies have determined that FMDV 2B reduced the expression of RIG-I, LGP2, and nucleotide-binding oligomerization domain (NOD) 2 proteins to facilitate viral replication (Zhu *et al.* 2016, 2017; Liu *et al.* 2019). FMDV 2C is a highly conserved viral protein in all the serotypes of FMDV. It contains a predicted amphipathic helix (residues 17–34) and a conserved ATPase domain formed by residues 60–270, which improves the ability to bind to cell membranes, membrane rearrangement, and formation of the viral replication complex (Sweeney *et al.* 2010; Wang *et al.* 2012; Zheng

Huisheng Liu and Qiao Xue have contributed equally to this work.

Electronic supplementary material The online version of this article (https://doi.org/10.1007/s12250-020-00322-2) contains supplementary material, which is available to authorized users.

✉ Haixue Zheng
haixuezheng@163.com

[1] State Key Laboratory of Veterinary Etiological Biology, National Foot and Mouth Diseases Reference Laboratory, Key Laboratory of Animal Virology of Ministry of Agriculture, Lanzhou Veterinary Research Institute, Chinese Academy of Agricultural Sciences, Lanzhou 730046, China

et al. 2014). In addition, the biological significance of the 2C–beclin1 and 2C–vimentin interactions have been identified (Gladue *et al.* 2012, 2013). Our previous results have demonstrated that FMDV 2B and 2C interacts with NOD2 and reduces its protein expression to promote viral replication (Liu *et al.* 2019).

NOD2, a widely studied member belong to the nucleotide-binding oligomerization domain-like receptors (NLRs) family, can recognize muramyl dipeptide (MDP) and then activates nuclear factor-κB (NF-κB) signaling pathway (Kanneganti *et al.* 2007; Shaw *et al.* 2008; Cavallari *et al.* 2017). However, recent studies showed that some viruses also activate NOD2 (Sabbah *et al.* 2009; Vissers *et al.* 2012; Nystrom *et al.* 2013; Kapoor *et al.* 2014; Al Nabhani *et al.* 2017; Dominguez-Martinez *et al.* 2018). The activated NOD2 interacts with mitochondrial antiviral-signaling protein (MAVS), leading to the activation of interferon (IFN) regulatory factor 3 (IRF3) to produce IFN. In addition, the activation of NOD2 also triggers NF-κB pathway during viral infection (Al Nabhani *et al.* 2017).

Receptors interaction protein 2 (RIP2, also called CARD3, RICK, or CARDIAK) contains a caspase-recruitment domain (CARD) that mediates the interaction with other CARD-containing proteins including NOD2. NOD2 interacts with RIP2 during viral infection, leading to the activation of NF-κB (Nembrini *et al.* 2009; Wu *et al.* 2018; Zheng *et al.* 2018). In addition, phosphorylation of RIP2 is identified as a marker for activation of NOD2-mediated NF-κB pathway (Jing *et al.* 2014).

To date, the impact of NOD2 on FMDV infection has been reported (Liu *et al.* 2019). However, the role of RIP2 during FMDV infection remains unknown. In the present study, we investigated the role of RIP2 during FMDV infection and determined that RIP2 was involved in activation of innate immune signal pathways during FMDV infection. We determined the antiviral effect of RIP2 against FMDV. We also identified novel antagonistic mechanisms mediated by FMDV 2B, 2C, $3C^{pro}$, and L^{pro} proteins to inhibit RIP2-mediated antiviral effect.

Materials and Methods

Cells, Viruses and Infection

Porcine kidney 15 (PK-15) cells, green monkey kidney cell line (Vero), and Human embryonic kidney 293T (HEK-293T) cells were cultured in Dulbecco's modified Eagle medium (Gibco) supplemented with 10% heat-inactivated fetal bovine serum (FBS) (Gibco) and maintained at 37 °C (5% CO_2). FMDV type O strain O/BY/CHA/2010 and type A strain A/HuBWH/CHA/2009 were used for viral challenge. SVV and EV71 strains were prepared in our laboratory (Xue *et al.* 2018). Viral infection experiments were carried out as described previously (Zheng *et al.* 2013).

Plasmids and Antibodies

The cDNA of RIP2 and PABPC1 were cloned into the p3xFLAG-CMV-10 vector (Sigma-Aldrich) to yield the FLAG-tagged expression construct (FLAG-RIP2 and FLAG-PABPC1). Each of FMDV full-length viral cDNA was inserted into p3xFLAG-CMV-7.1 vector (Sigma-Aldrich) to construct plasmids expressing FLAG-tagged viral proteins. A series of FLAG-tagged truncated 2B constructs were prepared in our laboratory (Zhu *et al.* 2016). A series of FLAG-tagged truncated 2C constructs were prepared as described previously (Sweeney *et al.* 2010; Liu *et al.* 2019). $3C^{pro}$ mutants without protease activity were prepared in our laboratory (Li *et al.* 2017). A series of L^{pro} mutants without protease activity were prepared as described previously (Wang *et al.* 2011). Porcine IFN-β and NF-κB promoter luciferase reporter plasmids (IFN-β-Luc and NF-κB-Luc) were prepared in our laboratory (Liu *et al.* 2019). All constructed plasmids were confirmed by DNA sequencing.

The commercial antibodies used in this study include: anti-FLAG monoclonal antibody (Santa Cruz Biotechnology), anti-FLAG polyclonal antibody (Sigma-Aldrich), anti-PABPC1 polyclonal antibody (Cell Signaling Technology), anti-P65 monoclonal antibody (Cell Signaling Technology), anti-P-P65 monoclonal antibody (Cell Signaling Technology), anti-IRF3 monoclonal antibody (Cell Signaling Technology), anti-P-IRF3 monoclonal antibody (Cell Signaling Technology), anti-RIP2 monoclonal antibody (Cell Signaling Technology), anti-PKR monoclonal antibody (Cell Signaling Technology), anti-MX1 monoclonal antibody (Cell Signaling Technology), and anti-β-actin monoclonal antibody (Santa Cruz Biotechnology). Anti-VP1 and 2C polyclonal antibody was prepared in our laboratory (Li *et al.* 2017; Liu *et al.* 2019).

Reporter Gene Assays

The reporter gene assays were performed as described previously (Liu *et al.* 2019). Briefly, PK-15 cells were co-transfected with 0.1 μg/well of IFN-β-Luc or NF-κB-Luc along with 0.01 μg/well of pRL-TK Renilla luciferase reporter plasmid and RIP2 or NC siRNA. At 36 h post-transfection (hpt), PK-15 cells were mock infected or infected with FMDV (MOI=1.5). MDP (Sigma-Aldrich) stimulation was used as a control. At 6 hpi, the dual-specific luciferase assay kit (Promega) was used to analyze the firefly and Renilla luciferase activities according to the manufacturer's instruction. The data represent the means

and standard deviations from three independent experiments.

Co-IP and Western Blotting

PK-15 cells cultured in 10-cm dishes were transfected with vairous plasmids or infected with FMDV. Cells were lysed and immunoprecipitated as described previously (Li *et al.* 2016; Liu *et al.* 2018, 2018). The target proteins were resolved by 10% SDS-PAGE and transferred onto an Immobilon-P membrane (Millipore, Bedford, MA, USA). The membrane was blocked with 5% skim milk at room temperature for 2 h, and then incubated with primary and secondary antibodies as described previously (Zhu *et al.* 2013). The antibody–antigen complexes were visualized using enhanced chemiluminescence detection reagents (Thermo Fisher Scientific Inc., Rockford, IL, USA).

Knockdown of RIP2 Using siRNA

siRNA used in this study was synthesized by Gene Pharma (Shanghai, China). Knockdown of RIP2 in PK-15 cells was carried out by transfection of RIP2 siRNA using Lipofectamine 2000 (Invitrogen) according to the manufacturer's instruction. NC siRNA was used as a negative control. The porcine RIP2 siRNA sequence was F: 5′-CCUGAUGUUCCUUGGCCUUTT-3′, R: 5′-AAGGCCAAGGAACAUCAGGTT-3′ (Zhu 2018).

RNA Extraction and qPCR

Total RNA and cDNA were prepared as described previously (Zhu *et al.* 2016). The glyceraldehyde-3-phosphate dehydrogenase (GAPDH) gene was used as an internal control. Relative fold change of mRNA was calculated based on the comparative cycle threshold (CT) ($2^{-\Delta\Delta CT}$) method (Schmittgen and Livak 2008). The qPCR primers used in this study are listed in Supplementary Table S1. The porcine RIP2 qPCR primers were described previously (Jing *et al.* 2014).

Proteasome, Lysosome and Caspase Inhibitors Assay

PK-15 cells cultured in six-well plates were incubated with FMDV or serum-free medium for 2 h. After that, cells were maintained in fresh medium supplemented with 1% FBS in the presence or absence of proteasome inhibitor MG132 (10 μmol/L or 20 μmol/L) (Merck & Co., Kenilworth, NJ, USA), caspase inhibitor Z-VAD-FMK (10 or 50 μmol/L) (Sigma), or lysosome inhibitor CQ (50 or 100 μmol/L) (Sigma) for 12 h, and then were collected for western blotting analysis.

MTS Assay

The MTS assay was performed to evaluate the cytotoxicity of MG132, CQ, and Z-VAD-FMK on cells according to the manufacturer's instruction. The experiments were repeated three times.

Statistical Analysis

Statistical analysis was performed using SPSS Statistics for Windows, Version 17.0 (SPSS Inc., Chicago, IL, USA). The student's *t* test was used for a comparison of three independent experiments. A $*P$ value<0.05 was considered statistically significant; A $**P$-value<0.01 was considered statistically highly significant.

Results

RIP2 was Involved in the Activation of Innate Immune Signal Pathways During FMDV Infection

To study the involvement of RIP2-mediated innate immune signal pathways during FMDV infection, PK-15 cells were transfected with IFN-β-Luc, or NF-κB-Luc, and pRL-TK *Renilla* luciferase reporter plasmid along with RIP2 small interfering RNA (siRNA) or negative control (NC) siRNA. At 36 h post-transfection (hpt), the transfected cells were stimulated by MDP, mock infected or infected with FMDV at a multiplicity of infection (MOI) of 1.5 for 6 h. The FMDV-induced activation of IFN-β or NF-κB promoter was determined by dual-specific luciferase assay kit. MDP induced activation of NF-κB promoter, whereas it did not induce activation of IFN-β promoter. Knockdown of RIP2 significantly inhibited FMDV-triggered IFN-β and NF-κB signal pathways activation (Fig. 1A, 1B). Reduction of RIP2 also significantly abrogated MDP-induced activiation of NF-κB signal pathway (Fig. 1B).

Phosphorylation of p65 and IRF3 is considerd as a maker for NF-κB and IFN-β pathways, respectively (Liu *et al.* 2018; Tian *et al.* 2018). To further confirm the role of RIP2 during FMDV infection, the phosphorylation status of p65 and IRF3 was deterimined. PK-15 cells were transfected with the RIP2 siRNA or NC siRNA for 36 h. The cells were then infected with FMDV (MOI=0.5). Viral protein (VP1) and the indicated host proteins in the RIP2 and NC siRNA cells were detected and compared. The results showed that the phosphorylation of endogenous p65 and IRF3 induced by FMDV infection was impaired in the RIP2 siRNA cells compared with that in the NC siRNA cells (Fig. 1C).

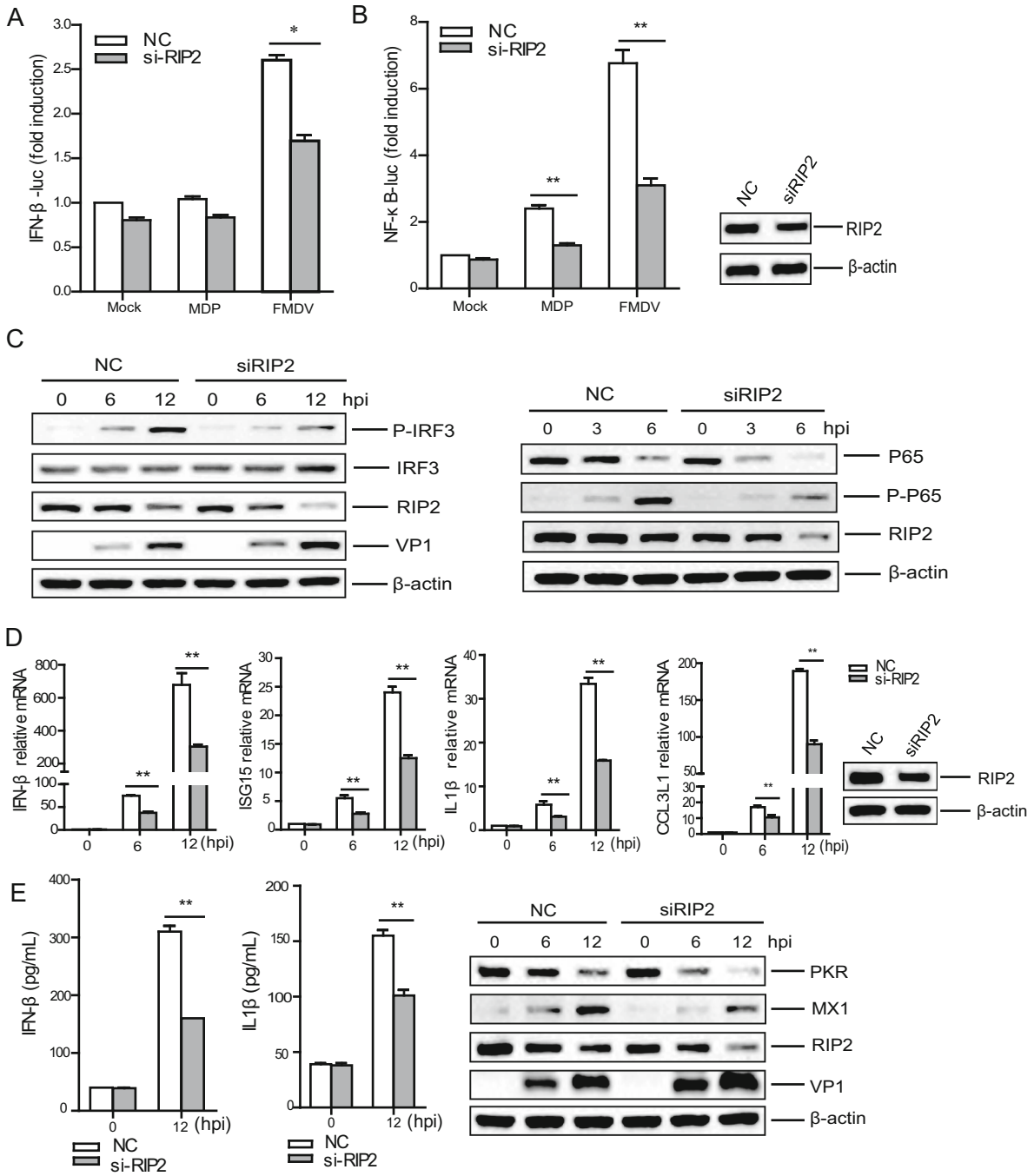

Fig. 1 RIP2 was involved in FMDV infection-mediated innate immune signaling pathways. **A**, **B** PK-15 cells cultured in 24-well plates were co-transfected with 0.1 μg/well of IFN-β-Luc or NF-κB-Luc, 0.01 μg/well of pRL-TK plasmid, and 75 nmol/L per well of RIP2 or NC siRNA for 36 h. Cells were stimulated by MDP (5 μg/mL) or mock-infected or infected with FMDV (MOI=1.5) for 6 h. The promoter activity of IFN-β (**A**) or NF-κB (**B**) was determined by the dual-specific luciferase assay kit. The knockdown of RIP2 was confirmed by Western blotting. **C** PK-15 cells cultured in 3.5 cm dishes were transfected with the 150 nmol/L of RIP2 siRNA or NC siRNA for 36 h. Then, the cells were mock-infected or infected with FMDV (MOI=0.5). The cells were collected at 0, 3, 6, or 12 h after infection. The target proteins were detected by Western blotting. **D** Similar transfection and infection experiments were performed as described above. The cells were collected for RNA extraction. The IFN-β, ISG15, IL1β, and CCL3L1 mRNA levels were determined by qPCR assay. GAPDH was used as an internal control. **E** Similar transfection and infection experiments were performed as described above. The supernatant were collected for detecting IFN-β and IL1β protein expression using ELISA kit, and the cells were collected for detecting PKR and MX1 protein expression by Western blotting. All the results represent the means and standard deviations of data. $^{**}P<0.01$ versus negative control.

To further investigate whether down-regulation of RIP2 affects IFN-β, IFN-stimuated genes (ISGs), and proinflammatory cytokines expression during FMDV infection, we compared the mRNA and protein levels of these genes in the RIP2 and NC siRNA cells after infected with FMDV. The mRNA expression of IFN-β, ISG15, IL1β, and CCL3L1 were significantly decreased in the RIP2 siRNA cells compared with that in the NC siRNA cells (Fig. 1D). The proteins expression of IFN-β, IL1β, PKR, and MX1 were also decreased in the RIP2 siRNA cells compared with that in the NC siRNA cells (Fig. 1E). Taken together, these results indicated that FMDV infection triggered RIP2-mediated IFN-β and NF-κB pathways activation; and downregulation of RIP2 significantly impaired the activation of IFN-β and NF-κB pathways during FMDV infection.

RIP2 Inhibited FMDV Replication During Viral Infection

To determine the impact of RIP2 on FMDV replication, we evaluated the production of FMDV in PK-15 cells transfected with different dose of FLAG–RIP2-expressing plasmid. At 24 hpt, the cells were infected with FMDV (MOI=0.5). The viral RNA, viral titers, and protein abundance were compared. Over-expression of RIP2 significantly suppressed FMDV yield in a dose-dependent manner (Fig. 2A).

Replication of FMDV in PK-15 cells transfected with the RIP2 siRNA or NC siRNA was also assessed. At 36 hpt, the cells were infected with equal amounts of FMDV (MOI=0.5). Viral RNA, VP1 protein, titers, and host RIP2 protein in the RIP2 siRNA and NC siRNA cells were compared after FMDV infection. FMDV replication was significantly enhanced in the RIP2 siRNA cells compared with that in NC siRNA cells (Fig. 2B). These results demonstated the important antiviral role of RIP2 against FMDV.

FMDV Infection Triggered RIP2 Transcription and Decreased Its Protein Expression

To explore the state of RIP2 in FMDV-infected cells, PK-15 cells were infected with FMDV and the dynamics of RIP2 were evaluated. The expression level of RIP2 mRNA was significantly upregulated as the viral infection progressed (Fig. 3A), whereas the abundance of RIP2 protein was gradually decreased and no cleaved bands were observed (Fig. 3B). The expression of RIP2 in the mock-infected cells was also investigated. There was no significant variation for RIP2 mRNA or protein levels in the mock-infected cells (Supplementary Fig. S1).

In the present study, a commercial anti-RIP2 antibody that detects the carboxyl terminal regions of RIP2 was used in the Western blotting analysis. To detect the N terminal region of RIP2, PK-15 cells were transfected with N terminal FLAG-tagged RIP2 plasmid. At 24 hpt, the cells were infected with FMDV. The target proteins were analyzed by Western blotting using anti-FLAG antibody. Again, the expression of RIP2 was remarkably decreased and no cleaved bands were observed in the FMDV-infected cells (Fig. 3C).

To confirm the impact of different FMDV strains on the expression of RIP2 protein, PK-15 cells were infected with FMDV type O or A strains (MOI=0.5). The expression of RIP2 protein was determined by Western blotting. Both FMDV type O and A strains reduced RIP2 protein expression (Fig. 3D). Taken together, these results indicated that FMDV infection triggered RIP2 transcription but reduced its protein expression.

FMDV, Seneca Valley virus (SVV), and enterovirus 71 (EV71) belong to the family of *Picornaviridae*. Thus, we also assessed the impact of SVV and EV71 on RIP2 expression. EV71 infection reduced RIP2 protein expression (Fig. 3E). However, SVV infection did not affect the expression of RIP2 protein (Fig. 3E).

Five different RIPs, including RIP, RIP2, RIP3, RIP4 and RIP5, have been described in RIP family. RIPs interact with the tumor necrosis factor receptor (TNFR) family proteins and regulate the NF-kB pathway as well as cellular apoptosis (Adams *et al.* 2007; Kopparam *et al.* 2017; Cai *et al.* 2018). To investigate whether FMDV infection decreased other important RIP family members, we also detected the dynamics of the widely-studied RIP and RIP3 proteins (Huang *et al.* 2019). FMDV reduced both RIP and RIP3 proteins expression as the viral infection progressed (Fig. 3F). In contrast, no significant changes of RIP and RIP3 protein levels were observed in the mock-infected cells (data not shown).

FMDV 2B, 2C, $3C^{pro}$, and L^{pro} Proteins were Responsible for the Reduction of RIP2

To investigate the viral proteins that were responsible for the reduction of RIP2, PK-15 cells were transfected with the plasmids expressing various FLAG-tagged viral proteins. The endogenous RIP2 protein was detected by Western blotting. The expression of 2B, 2C, $3C^{pro}$, and L^{pro} protein significantly decreased RIP2 protein abundance (Fig. 4A). The 2B-, 2C-, $3C^{pro}$, and L^{pro}-induced reduction of endogenous RIP2 were further compared by performing the dose-dependent experiments (Fig. 4B). It showed that 2B-, 2C-, $3C^{pro}$, and L^{pro} reduced expression of RIP2 in a dose-dependent manner.

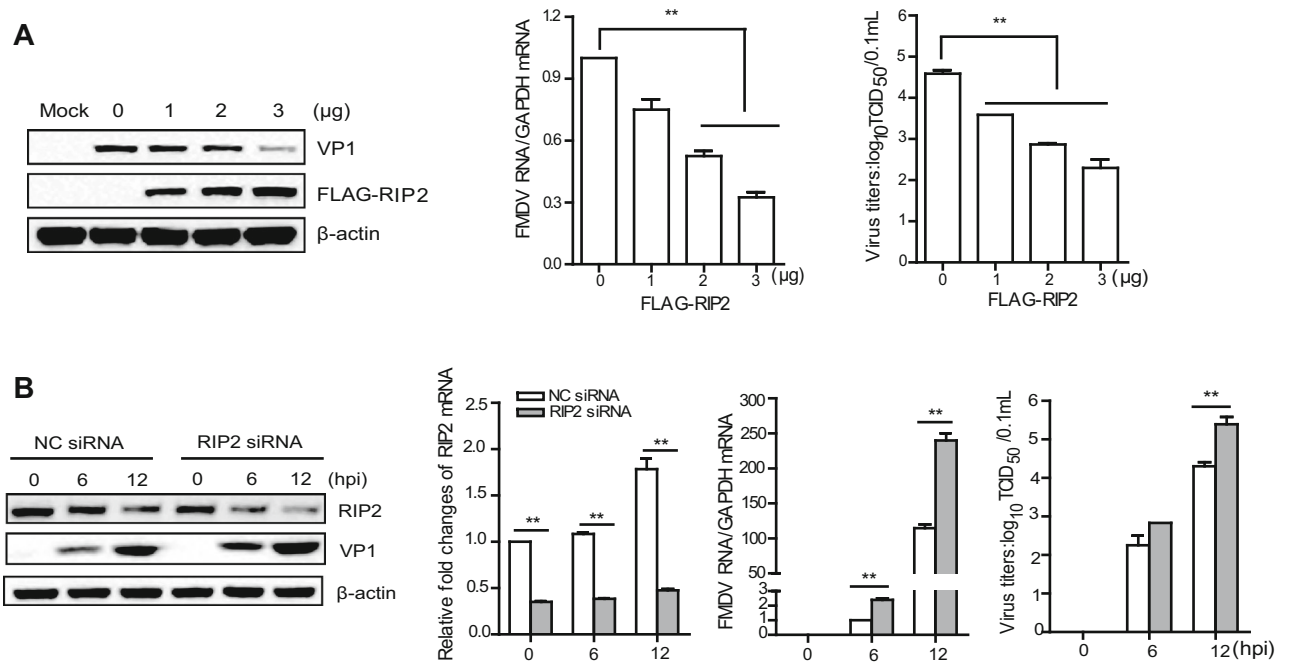

Fig. 2 RIP2 inhibited FMDV replication. **A** PK-15 cells cultured in six-well plates were transfected with 0, 1, 2, or 3 μg FLAG-RIP2-expressing plasmid or 3 μg empty FLAG vector. At 24 hpt, the cells were mock-infected or infected with FMDV (MOI=0.5) for 12 h. Expression of viral RNA was determined by qPCR assay; expression of the target proteins was detected by Western blotting, and viral titers were determined by $TCID_{50}$ assay. **B** PK-15 cells cultured in 3.5 cm dishes were transfected with 150 nmol/L NC siRNA or RIP2 siRNA for 36 h. Then, the cells were mock-infected or infected with FMDV (MOI=0.5) for 0, 6, and 12 h. Expression of viral RNA, VP1 protein, or viral titers were determined. All the results represent the means and standard deviations of data. GAPDH was used as an internal control. $^{**}P<0.01$ versus negative control.

The impact of 2B-, 2C-, $3C^{pro}$, and L^{pro} on the expression levels of RIP2 mRNA was also evaluated, which showed that 2B-, 2C-, $3C^{pro}$, and L^{pro} did not affect the mRNA levels of RIP2 (Fig. 4C). Together, these results suggested that the viral proteins 2B, 2C, $3C^{pro}$, and L^{pro} were responsible for the reduction of RIP2 protein.

Identification of the Functional Regions of 2B, 2C, $3C^{pro}$, and L^{pro} Responsible for the Reduction of RIP2

To determine whether the proteasomes, lysosomes or caspase-dependent pathways play roles in FMDV-, 2B-, 2C-, $3C^{pro}$, or L^{pro}-induced reduction of RIP2, the lysosome inhibitor chloroquine diphosphate (CQ), proteasome inhibitor MG132, and caspases inhibitor benzyloxycarbony (Cbz)-l-Val-Ala-Asp (OMe)-fluoromethylketone (Z-VAD-FMK) were used to assess the inhibitive effects of FMDV or the viral proteins on RIP2 protein expression. The cytotoxicity of the inhibitors was determined by MTS assay. All doses of the inhibitor used in the experiments did not induce significant cell death (Supplementary Fig. S2).

PK-15 cells were infected with FMDV (MOI=0.5) and maintained in the presence or absence of the inhibitors. At 12 h post-infection (hpi), expression of RIP2 was detected by western blotting. FMDV infection-induced reduction of RIP2 was not suppressed by MG132, CQ, or Z-VAD-FMK (Fig. 5A). The effects of MG132, CQ, or Z-VAD-FMK on 2B-, 2C-, $3C^{pro}$-, or L^{pro}-induced reduction of RIP2 were also examined. No inhibitory effects of MG132, CQ, or Z-VAD-FMK on reduction of RIP2 were observed (Supplementary Fig. S3). These results indicated that FMDV-, 2B-, 2C-, $3C^{pro}$-, or L^{pro}-induced reduction of RIP2 was independent of proteasomes, lysosomes, and caspases pathways.

To further confirm the functional domains of 2B, 2C, $3C^{pro}$, and L^{pro} that were essential for reduction of RIP2, a series of truncated mutants of FMDV 2B and 2C were used for detailed analysis (Fig. 5B). $3C^{pro}$ mutants without the protease activity (H46Y, D84N, and C163G) were used for detailed analysis. The $3C^{pro}$ mutant with the protease activity (H205R) was used as a control. L^{pro} has protease activity (papainlike proteinase) and SAP (for SAF-A/B, Acinus, and PIAS) domain between amino acids 47 and 83. Therefore, L^{pro} mutants without the protease activity (C51A, D163N, and D164N) and L^{pro} SAP-domain-deficient mutants (I83A or I86A) were used for detailed analysis. FLAG–2B, FLAG–2C, FLAG–3C, FLAG–L, or their mutants expressing plasmids were transfected into PK-15 cells, separately. At 24 hpt, the abundance of RIP2

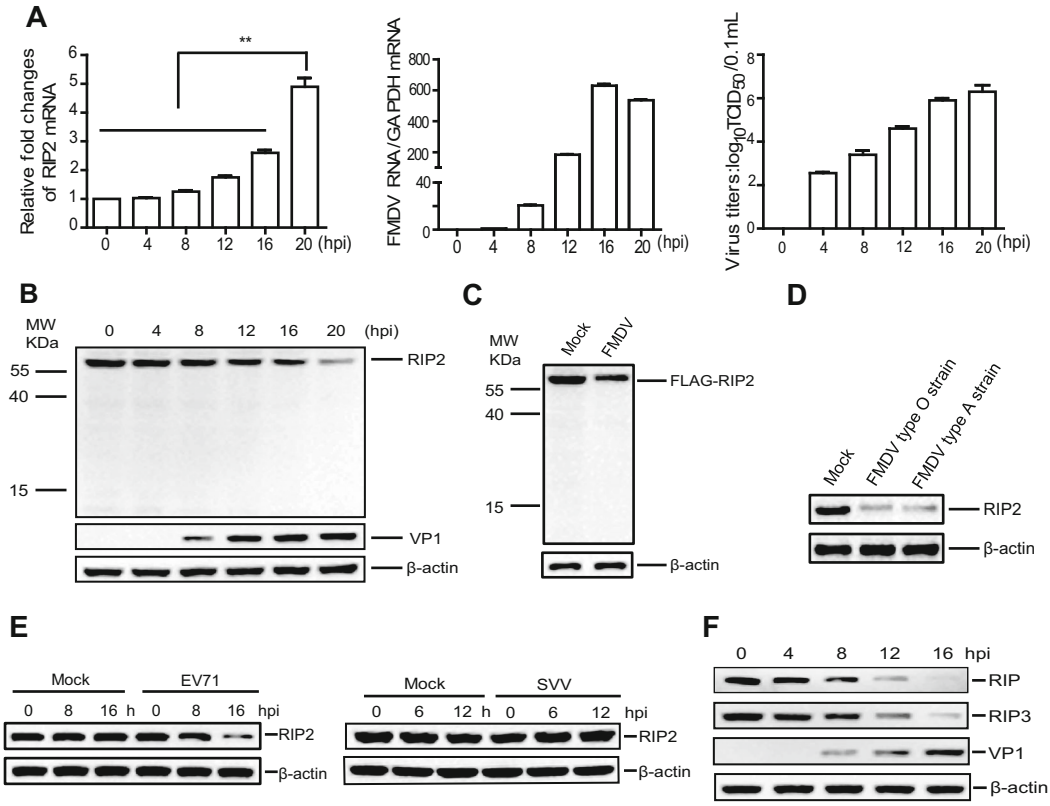

Fig. 3 FMDV infection reduced the expression of RIP2 protein. PK-15 cells cultured in 3.5 cm dishes were mock-infected or infected with FMDV (MOI=0.5). The cells were collected and analyzed at the indicated time points. Expression of viral RNA and RIP2 mRNA was determined by qPCR assay, and viral titers were determined by $TCID_{50}$ assay (**A**). GAPDH was used as an internal control. **B** Expression of RIP2 and VP1 was detected by Western blotting. **C** PK-15 cells cultured in 3.5 cm dishes were transfected with 2 μg FLAG-RIP2-expressing plasmid. At 24 hpt, the cells were mock-infected and infected with FMDV (MOI 0.5) for 12 h. Expression of the target proteins were detected by western blotting. **D** PK-15 cells were mock-infected or infected with FMDV type O or A strains (MOI =0.5) for 12 h. Expression of endogenous RIP2 protein was detected by western blotting. **E** Vero cells were mock-infected or infected with EV71 (MOI=1) for 0, 8, and 16 h (left). HEK-293T cells were mock-infected or infected with SVV (MOI=1) for 0, 6, and 12 h (right). Expression of the RIP2 protein was detected by western blotting. **F** PK-15 cells were mock-infected or infected with FMDV (MOI= 0.5). The cells were collected and analyzed at 0, 4, 8, 12, 16 h after infection. Expression of the target proteins was detected by Western blotting. All the results represent the means and standard deviations of data. $^{**}P<0.01$ versus negative control.

was detected by Western blotting. The deletion of the carboxyl terminal 105–114 or 135–144 regions of 2B abrogated the reduction of RIP2 (Fig. 5C), which was in accordance with that the 2B-induced reduction of RIG-I and NOD2 (Liu *et al.* 2019). The deletion of the N terminal 1–34, 1–38, 1–52, or 1–61 regions of 2C did not induce the reduction of RIP2 (Fig. 5D). N terminal (resides 17–34) of FMDV 2C has a predicted amphipathic helix and exerts various roles (Sweeney *et al.* 2010). Therefore, we speculate that 2C-induced reduction of RIP2 is dependent on amphipathic helix. All the $3C^{pro}$ mutants with abrogated protease activity failed to induce the reduction of RIP2 (Fig. 5E). The L^{pro} mutant (C51A) with abrogated protease activity failed to induce the reduction of RIP2, whereas the mutation of SAP domain did not affect L^{pro}-induced reduction RIP2 protein (Fig. 5F). These results indicated that $3C^{pro}$ and L^{pro} reduced RIP2 protein expression depended on their protease activity. 2B deceased RIP2 through its C-terminus region and 2C deceased RIP2 by its N-terminus region.

FMDV 2C Interacted with RIP2

FMDV 2B, $3C^{pro}$, and L^{pro} have been widely reported to perform antagonistic roles by inducing the reduction or cleavage of many host proteins during FMDV infection (Wang *et al.* 2011; Zhu *et al.* 2016, 2017; Feng *et al.* 2018; Liu *et al.* 2019). However, the 2C-induced antagonistic mechanism remains unknown. Therefore, FMDV 2C was selected for further study. To explore a possible interaction between RIP2 and 2C, PK-15 cells were transfected with FLAG–2C-expressing plasmid or empty vector. Cells lysates were immunoprecipitated with anti-RIP2 antibody and analyzed by Western blotting. RIP2 pulled down FLAG–2C, which indicated that 2C interacted with RIP2 (Fig. 6A). A reverse immunoprecipitation experiment was

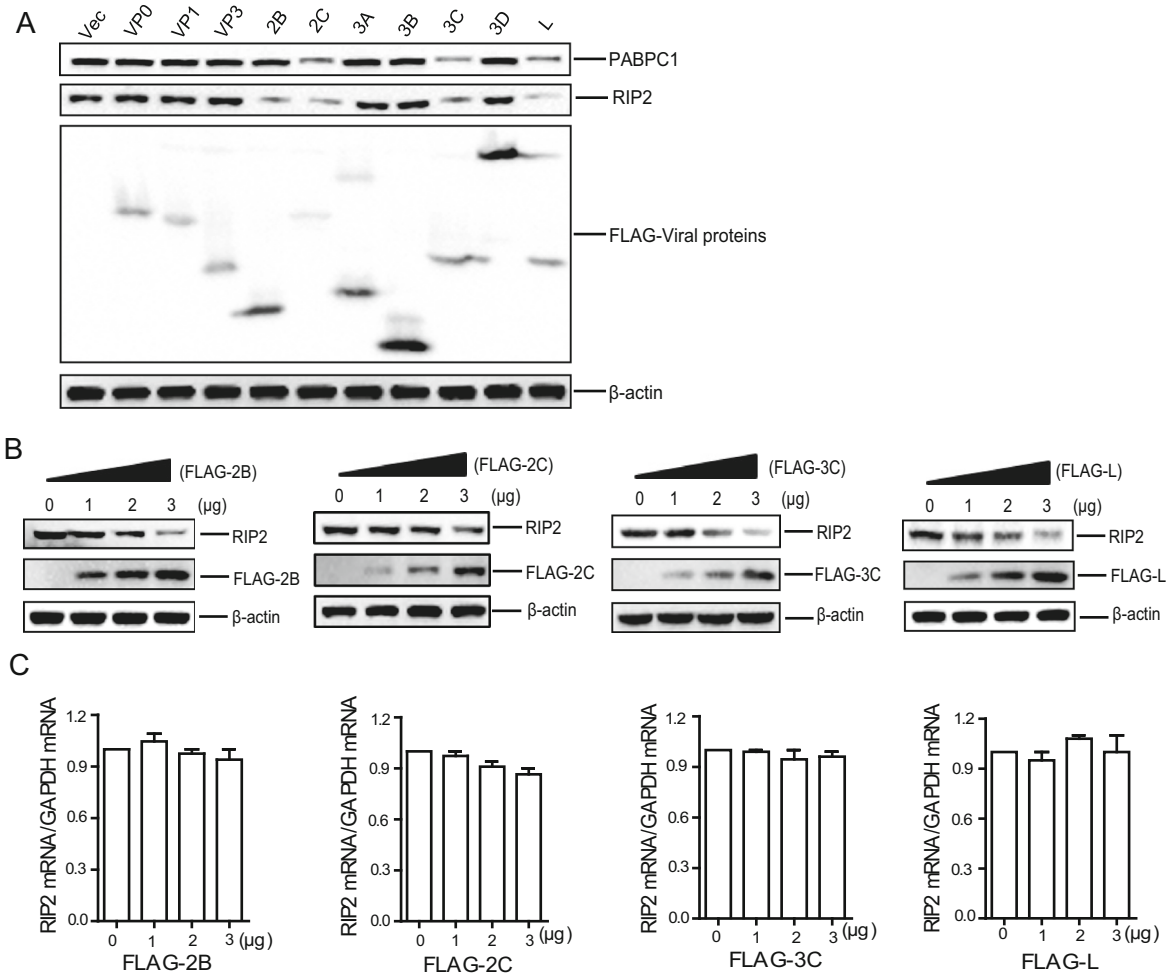

Fig. 4 FMDV 2B, 2C, $3C^{pro}$, and L^{pro} proteins induced the reduction of RIP2. **A** PK-15 cells cultured in six-well plates were transfected with 2 μg plasmid expressing FLAG-tagged viral proteins. At 24 hpt, expression of endogenous RIP2 and PABPC1 proteins were determined by western blotting. **B**, **C** PK-15 cells cultured in six-well plates were transfected with 0, 1, 2, and 3 μg FLAG-2B-, FLAG-2C-, FLAG-3C-, or FLAG-L-expressing plasmids for 24 h. Expression of the RIP2 and viral proteins was detected by Western blotting (**B**); expression of RIP2 mRNA was determined by qPCR assay (**C**). GAPDH was used as an internal control. All the results represent the means and standard deviations of data.

also performed, which showed that FLAG–2C immunoprecipitated RIP2 (Fig. 6B).

To further investigate the interaction between RIP2 and 2C in the context of viral infection, PK-15 cells were mock-infected or infected with FMDV. Cell lysates were immunoprecipitated with anti-RIP2 antibody and analyzed by immunoblotting. RIP2 pulled down 2C in FMDV-infected cells (Fig. 6C). A reverse immunoprecipitation experiment was subsequently performed using anti-2C antibody, which showed that 2C also immunoprecipitated host RIP2 protein (Fig. 6D).

We further identified the crucial regions of 2C that is essential for 2C-RIP2 interaction. PK-15 cells were transfected with FLAG–2C-expressing plasmid, FLAG–2C mutant plasmids, or empty vector. Cells ysates were immunoprecipitated with anti-FLAG antibody and analyzed by western blotting. FLAG–2C pulled down RIP2. The 2C mutants with deletion of the N terminal 1–34, 1–38, 1–52, or 1–61 regions did not interact with RIP2 (Fig. 6E). Taken together, these results indicated that the 2C-RIP2 interaction was involved in inducing the reduction of RIP2 expression, and the N terminal region of 2C was essential for the interaction between 2C and RIP2.

FMDV 2C Induced the Reduction of PABPC1 Protein, and Downregulation of PABPC1 Reduces the Expression of RIP2

FMDV 2C induces the reduction of host NOD2 protein, which is independent of the cleavage of host eIF4G, induction of cellular apoptosis, and proteasomes, lysosomes, or caspases pathways (Liu *et al.* 2019). The

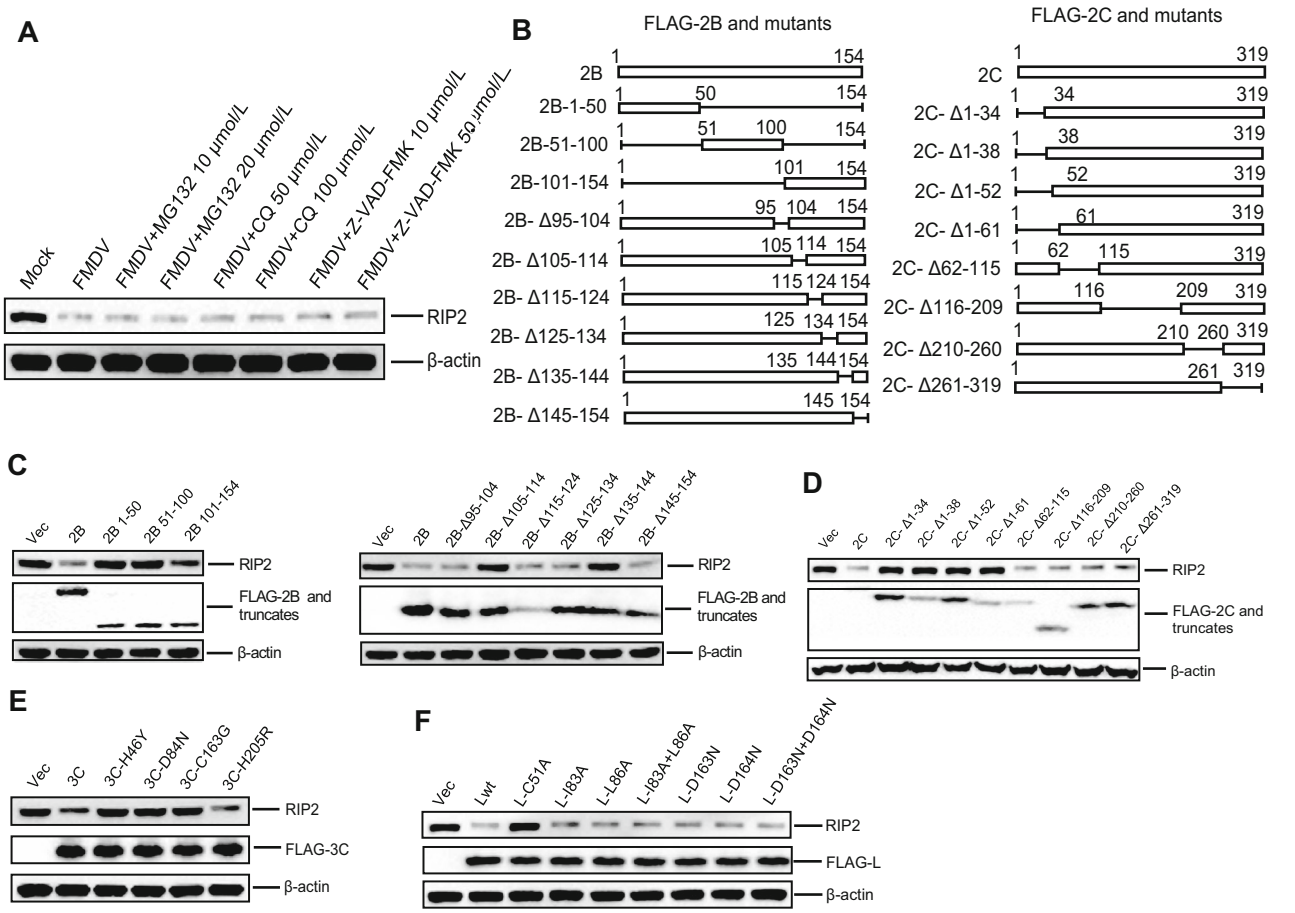

Fig. 5 The functional regions of 2B, 2C, $3C^{pro}$, and L^{pro} responsible for reduction of RIP2. **A** The experiment was performed as "materials and methods" described. **B** Schematic representation showing a series of FLAG-tagged truncated 2B and 2C mutants. **C**, **D**, **E**, **F** PK-15 cells cultured in six-well plates were transfected with 1.5 μg FLAG-2B-, FLAG-2C-, FLAG-3C-, FLAG-L-, or their mutant expressing plasmids for 24 h. The cells were collected and analyzed by Western blotting.

mechanism by which FMDV 2C inhibit host proteins expression remains unknown. To explore the involved mechanism, an important host eukaryotic translation initiation factor poly(A) binding protein cytoplasmic 1 (PABPC1, also known as PABP or PABP1) (Kuyumcu-Martinez *et al.* 2004; Copeland *et al.* 2013; Eliseeva *et al.* 2013; Copsey *et al.* 2017; Sun *et al.* 2017) was selected for further study. PABPC1 promotes host protein translation initiation by interacting with eIF4G (Smith *et al.* 2017). It has been widely reported that many viruses cleave PABPC1 to inhibit host proteins synthesis (Kobayashi *et al.* 2012).

Here, we evaluated the effect of FMDV infection on the expression of endogenous PABPC1. Our results showed that the expression of PABPC1 was gradually decreased as infection progressed and no cleaved bands were observed (Fig. 7A). A commercial anti-PABPC1 antibody that detects the carboxyl terminal regions of PABPC1 was used for the detection of endogenous PABPC1. To detect the N terminal region of PABPC1, PK-15 cells were transfected with N terminal FLAG-tagged PABPC1 plasmid. At 24 hpt, the cells were infected with FMDV. The PABPC1 protein was analyzed by Western blotting using anti-FLAG antibody. The N terminal cleaved bands of PABPC1 were clearly observed in the FMDV-infected cells (Fig. 7B).

We further evaluated the effect of FMDV proteins on the expression of PABPC1, and our results showed that FMDV 2C and $3C^{pro}$ significantly reduced the expression of PABPC1 protein and no cleaved bands were observed (Figs. 4A and 7C), and FMDV L^{pro} cleaved PABPC1 protein. These results were in accordance with previous results that FMDV infection and overexpression of FMDV L^{pro} induced cleavage of PABPC1 protein (Rodriguez Pulido *et al.* 2007). However, we for the first time showed that FMDV 2C and $3C^{pro}$ reduced PABPC1 protein expression. Therefore, the 2C- and $3C^{pro}$-induced reduction of endogenous PABPC1 was further confirmed by performing dose-dependent experiments in PK-15 cells, which indicated that both 2C and $3C^{pro}$ reduced the expression of PABPC1 in a dose-dependent manner

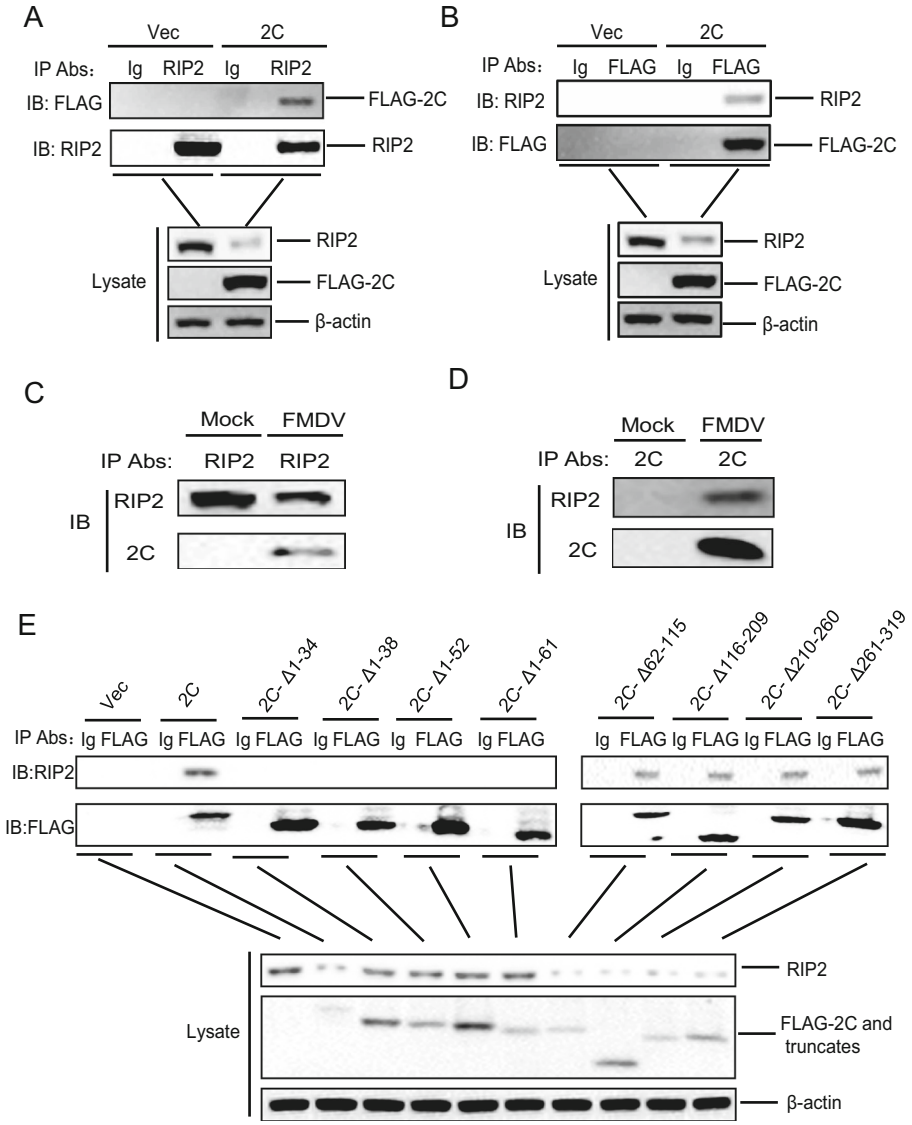

Fig. 6 RIP2 interacted with FMDV 2C. **A** PK-15 cells were transfected with 10 μg FLAG–2C expressing plasmid or 10 μg empty FLAG vector. At 30 hpt, cells lysates were immunoprecipitated with anti-RIP2 antibody and subjected to western blotting. The whole-cell lysates and IP antibody-antigen complexes were analyzed by IB using anti-RIP2, anti-FLAG, or anti-β-actin antibodies. **B** Similar transfection in PK-15 cells and IP experiments were carried out as described above. However, the lysates were immunoprecipitated with anti-FLAG antibody. **C**, **D** PK-15 cells were mock-infected or infected with FMDV (MOI=0.5) for 12 h. The cells lysates were immunoprecipitated with anti-RIP2 antibody (**C**) or anti-2C antibody (**D**). The antibody-antigen complexes were detected using anti-RIP2 and anti-2C antibodies. **E** PK-15 cells were transfected with 10 μg empty FLAG vector, 10 μg FLAG–2C expressing plasmid, or 10 μg FLAG–2C mutants expressing plasmids. At 30 hpt, cells lysates were immunoprecipitated with anti-FLAG antibody and subjected to western blotting. The whole-cell lysates and immunoprecipitated antibody-antigen complexes were analyzed by IB using anti-FLAG, anti-RIP2, or anti-β-actin antibodies.

(Fig. 7D). The impact of 2C and $3C^{pro}$ on PABPC1 transcription was also evaluated, which indicated that 2C and $3C^{pro}$ did not disrupt the transcription of PABPC1 (Fig. 7E).

To explore whether the downregulation of PABPC1 potentially decreased abundance of RIP2, PK-15 cells were transfected with the PABPC1 siRNA or NC siRNA. At 36 hpt, the whole cell lysates were analyzed by Western blotting. Downregulation of PABPC1 induced the reduction of RIP2 (Fig. 7F).

Taken together, these results indicated that FMDV 2C and $3C^{pro}$ significantly decreased the expression of PABPC1 protein, which in turn resulting in the reduction of RIP2.

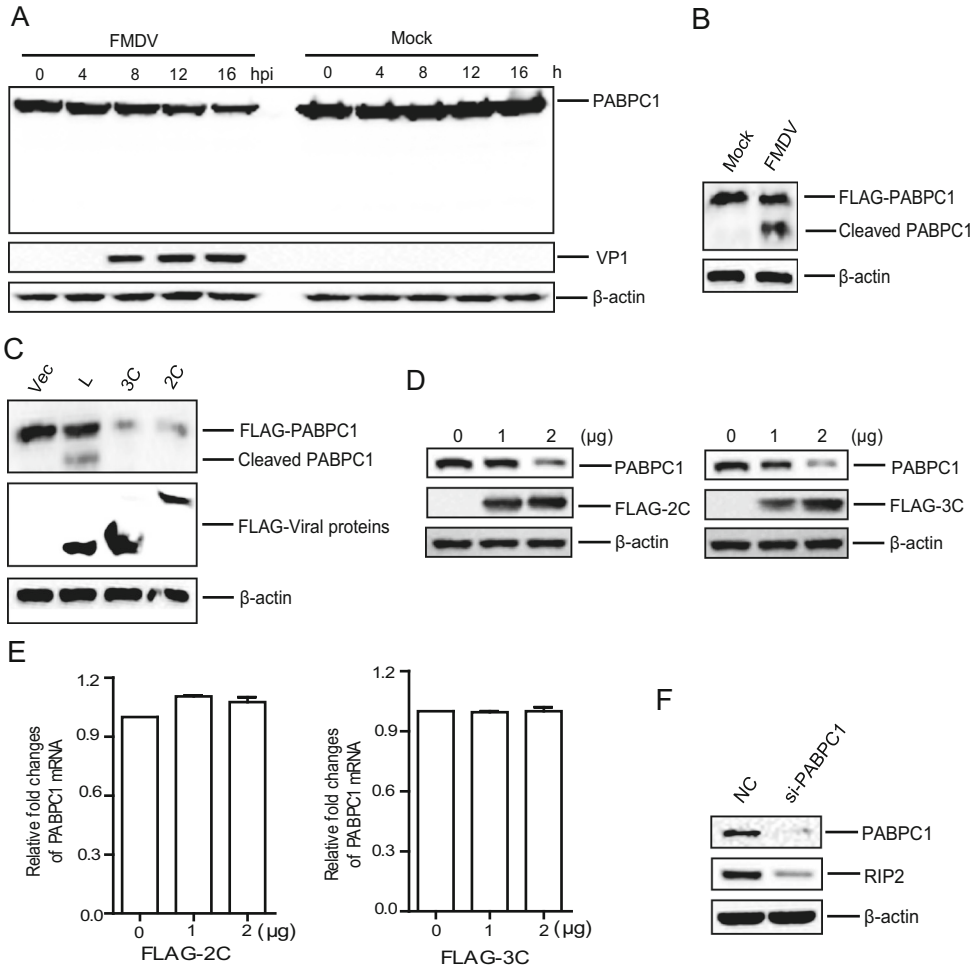

Fig. 7 FMDV 2C is responsible for the reduction of PABPC1 protein, and downregulation of PABPC1 reduces the expression of RIP2. **A** PK-15 cells cultured in 3.5 cm dishes were mock-infected or infected with FMDV (MOI 0.5). The cells were collected and analyzed at the indicated time points. Expression of PABPC1 and viral VP1 proteins was detected by western blotting. **B** PK-15 cells cultured in 3.5 cm dishes were transfected with 2 μg FLAG-PABPC1-expressing plasmid. At 24 hpt, the cells were mock-infected and infected with FMDV (MOI 0.5) for 12 h. Expression of the PABPC1 protein was detected by western blotting. **C** HEK-293T cells were transfected with 1.5 μg FLAG-2C-, FLAG-3C-, and FLAG-L-expressing plasmids along with 1.5 μg FLAG-PABPC1-expressing plasmid. At 24 hpt, the expression of the indicated proteins was detected by Western blotting. **D**, **E** PK-15 cells cultured in six-well plates were transfected with 0, 1, and 2 μg FLAG-2C- and FLAG-3C-expressing plasmids for 24 h. Expression of the target proteins were detected by western blotting (**D**). Expression of the PABPC1 mRNA level was deterimined by qPCR assay (**E**). GAPDH was used as an internal control. **F** PK-15 cells cultured in 3.5 cm dishes were transfected with 150 nmol/L NC siRNA or PABPC1 siRNA for 36 h. The whole cell lysates were analyzed by western blotting. All the results represent the means and standard deviations of data.

The Functional Regions or Sites of 2C and $3C^{pro}$ Responsible for Reduction of PABPC1

To identify the functional domains of 2C and $3C^{pro}$ that were essential for reduction of PABPC1, a series of mutants of FMDV 2C and $3C^{pro}$ were transfected into PK-15 cells. At 24 hpt, the abundance of PABPC1 was detected by Western blotting. It was observed that the deletion of N terminal 1–34, 1–38, 1–52, or 1–61 regions of 2C abrogated 2C-induced reduction of PABPC1 (Fig. 8A). All the $3C^{pro}$ mutants with the abrogated protease activity also failed to induce the reduction of PABPC1 (Fig. 8B), which indicated that $3C^{pro}$-induced reduction of PABPC1 by its protease activity. Taken together, these results indicated that the functional regions of 2C and $3C^{pro}$ responsible for reduction of PABPC1 were in accordance with that 2C- and $3C^{pro}$-induced reduction of RIP2.

Discussion

NOD2 senses the PAMPs derived from bacteria or viruses and play important roles in the immune response (Dominguez-Martinez *et al.* 2018; Egarnes and Gosselin 2018; Ren *et al.* 2018). RIP2, VISA, TBK1 IRF3, and P65 are the downstream molecules of NOD2-mediated

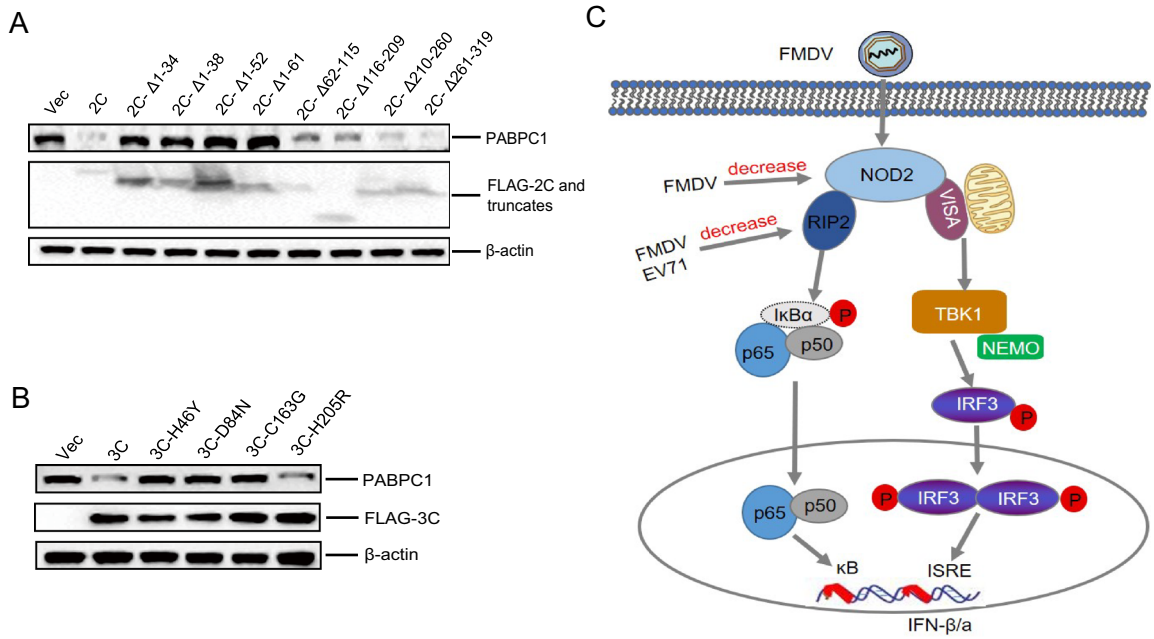

Fig. 8 The functional regions of 2C and $3C^{pro}$ responsible for decreasing the expression of PABPC1. **A**, **B** PK-15 cells cultured in six-well plates were transfected with 2 μg FLAG-2C-, FLAG-3C-expressing plasmids and mutant plasmids for 24 h. Expression of the PABPC1 protein was detected by western blotting. **C** Schematic representation showing the roles of NOD2- and RIP2-mediated IFN-β and NF-κB signaling pathways during FMDV infection and the involved antagonistic mechanisms.

signaling pathway (Sabbah *et al.* 2009). The impact of FMDV on NOD2, VISA, TBK1 IRF3, and P65 has been reported (Li *et al.* 2016; Fan *et al.* 2017; Liu *et al.* 2019). RIP2 is a specific adaptor molecule in NOD2-mediated signaling pathway (Nembrini *et al.* 2009). The relationship between FMDV and RIP2 remains unknown. In the present study, we explored the functions of RIP2 during FMDV infection and confirmed that RIP2 can regulate FMDV infection-mediated IFN-β and NF-κB signaling pathways.

The roles of NOD2 and RIP2 during viral infection have been described in several viruses (Al Nabhani *et al.* 2017). For instance, knockdown of NOD2 or RIP2 significantly decreases porcine reproductive and respiratory syndrome virus (PRRSV)-induced NF-κB signal pathway (Jing *et al.* 2014). NOD2 and RIP2 are involved in human cytomegalovirus (HCMV)-induced IFN-β and inflammatory cytokine (Kapoor *et al.* 2014). Here, our data showed that RIP2 was involved in FMDV-induced IFN-β and inflammatory cytokine production process. In addition, NOD2 inhibits HCMV, respiratory syncytial virus, and influenza A virus replication (Al Nabhani *et al.* 2017). The impact of RIP2 on viral replication remains unknown. Here, we for the first time determined the antiviral role of RIP2 against FMDV.

The expression of RIP2 protein severely affects NOD2-mediated signal pathways (Nembrini *et al.* 2009). To date, the regulation of RIP2 protein expression is rare reported (Lee *et al.* 2012). Our data showed that FMDV infection induced the reduction of RIP2, which may further affect the functions of NOD2. In addition, EV71 also decreased RIP2 protein expression, and SVV infection did not affect the expression of RIP2 protein, revealing different states of RIP2 during different picornaviruses infection. Together, the degradation of RIP2 is not specific for FMDV, and also not compatible for all picornaviruses.

Detailed analysis confirmed that FMDV 2B, 2C, $3C^{pro}$, and L^{pro} proteins can reduce abundance of RIP2. FMDV 2B reduces the abundance of host RIG-I (Zhu *et al.* 2016), LGP2 (Zhu *et al.* 2017), NOD2 (Liu *et al.* 2019), and RIP2, and the carboxyl terminal 105–114 and 135–144 regions of 2B are essential for the reduction of these proteins. However, the mechanism of 2B-induced reduction of host proteins remains unknown. FMDV $3C^{pro}$ and L^{pro} are well known as viral proteinases. $3C^{pro}$ and L^{pro} induce the cleavage of eIF4G or eIF4A to shut off host protein synthesis, leading to the reduction of many host proteins (Belsham *et al.* 2000; Wang *et al.* 2011). The protease activity of $3C^{pro}$ and L^{pro} palys important roles in pathogenic processes (Wang *et al.* 2011; Wang *et al.* 2012; Du *et al.* 2014; Fan *et al.* 2017; Li *et al.* 2017). In the present study, $3C^{pro}$ and L^{pro} also induce reduction of RIP2 through their protease activities, revealing novel antagonistic mechanisms evolved by FMDV $3C^{pro}$ and L^{pro}.

PABPC1 is an important regulator of translation initiation, mRNA deadenylation, mRNA decapping, mRNA stability, and mRNP maturation. In addition, PABPC1 also

promotes the joining of 60S ribosomal subunits to 48S preinitiation complexes to enhance the translation initiation (Christofori and Keller 1988; Sachs and Davis 1989; Vassalli *et al.* 1989; Sachs and Davis 1990; Wormington *et al.* 1996; Brown and Sachs 1998). The roles of PABPC1 during virus infection have been reported in several viruses. For instance, calicivirus 3C-like proteinase inhibits cellular translation by the cleavage of PABPC1 (Kuyumcu-Martinez *et al.* 2004); Picornavirus proteases, such as poliovirus $2A^{pro}$ and $3C^{pro}$ and coxsackievirus $2A^{pro}$, also cleaved PABPC1 to inhibit host proteins translation (Joachims *et al.* 1999; Kuyumcu-Martinez *et al.* 2002; Kuyumcu-Martinez *et al.* 2004; Bonderoff *et al.* 2008). Here, our results showed that FMDV 2C and $3C^{pro}$ induced reduction of PABPC1. Detailed analysis confirmed that $3C^{pro}$-induced reduction of PABPC1 depends on its protease activity, which showed that FMDV $3C^{pro}$ can also shut off host protein synthesis by decreasing PABPC1.

Host cellular mRNAs consist of 5′ 7-methylguanosine (m7G) cap structure, which can bind to the eIF4E, eIF4A, and eIF4G proteins (Avanzino *et al.* 2017). However, FMDV uses a cap-independent mechanism to promote viral protein synthesis by its own internal ribosome entry site (IRES) (Kanda *et al.* 2016). Many picornaviruses surpress host antiviral response and compete cellular translation factors by inhibiting host cell translation (Avanzino *et al.* 2017). Here, we for the first time showed that FMDV 2C reduced PABPC1 to inhibit host cell translation, resulting in decreased host antiviral response. Collectively, in addition to 3C and L^{pro}, FMDV 2C can shut off host protein synthesis.

FMDV 2BC palys an important role in the inhibition of the secretory pathway by inhibition of ER-to-Golgi transport (Moffat *et al.* 2005, 2007); Encephalomyocarditis virus 2C inhibited innate immune responses through interaction with MDA5 (Li *et al.* 2019); EV71 2C induced A3G degradation to regulate viral replication (Li *et al.* 2018). Our previous results have shown that FMDV 2C inhibited innate immune responses by reducing NOD2, however, the mechanism that 2C-induced reduction of NOD2 remains unknown (Liu *et al.* 2019). In the present study, our results further showed that FMDV 2C also reduced RIP2 protein expression, which is independent of induction of cellular apoptosis, the cleavage of eIF4G, and proteasome, lysosome, and caspases pathway, but is dependent of the amphipathic helix in the N terminal of 2C. Interestingly, FMDV 2C induced reduction of PABPC1 depends on amphipathic helix of 2C, which is consistent with that 2C-induced reduction of RIP2. Additionally, the reduction of PABPC1 potentially affected expression of RIP2. Collectively, these results showed that FMDV 2C inhibited the expression of RIP2 by decreasing PABPC1 protein level, revealing novel antagonize innate immune responses mechanism evolved by FMDV 2C. We speculated that 2C interacts with other host proteins to form a complex to degrade PABPC1. Thus, investigations of the proteinases that interact with 2C should be performed to understand the mechanisms by which it reduces the expression of PABPC1. FMDV 2B-induced reduction of RIP2 is independent of PABPC1, suggesting a PABPC1 protein-independent pathway for RIP2 reduction during FMDV infection. However, the mechanism of 2B-induced reduction of proteins remains unknown.

In conclusion, our results showed that RIP2 is involved in the activation of IFN-β and NF-κB signal pathways during FMDV infection, and RIP2 plays an antiviral role during FMDV infection. We also described for the first time the novel mechanisms by which FMDV 2B, 2C, $3C^{pro}$, and L^{pro} evolve to inhibit the RIP2-induced antiviral effect (Fig. 8C).

Acknowledgements This work was supported by Grants from the National Key R&D Programme of China (No. 2017YFD0501103 and 2017YFD0501800), the Key Development and Research Foundation of Yunnan (No. 2018BB004), and the Chinese Academy of Agricultural Science and Technology Innovation Project (CAAS-XTCX2016011-01 and Y2017JC55).

Author Contributions XL and HZ designed the experiments. HL, QX, and FY carried out the experiments. HL, WC, and ZZ, analyzed the data. HL and QX drafted the paper. HZ finalized the manuscript. All the authors approved the final manuscript.

Compliance with Ethical Standards

Conflict of interest The authors declare that they have no conflict of interest.

Animal and Human Rights Statement This study does not contain any studies with human participants or animals performed by any of the authors.

References

Adams S, Pankow S, Werner S, Munz B (2007) Regulation of NF-kappaB activity and keratinocyte differentiation by the RIP4 protein: implications for cutaneous wound repair. J Invest Dermatol 127:538–544

Al Nabhani Z, Dietrich G, Hugot JP, Barreau F (2017) Nod2: the intestinal gate keeper. PLoS Pathog 13:e1006177

Avanzino BC, Fuchs G, Fraser CS (2017) Cellular cap-binding protein, eIF4E, promotes picornavirus genome restructuring and translation. Proc Natl Acad Sci U S A 114:9611–9616

Belsham GJ (1993) Distinctive features of foot-and-mouth disease virus, a member of the picornavirus family; aspects of virus protein synthesis, protein processing and structure. Prog Biophys Mol Biol 60:241–260

Belsham GJ, McInerney GM, Ross-Smith N (2000) Foot-and-mouth disease virus 3C protease induces cleavage of translation

initiation factors eIF4A and eIF4G within infected cells. J Virol 74:272–280

Bonderoff JM, Larey JL, Lloyd RE (2008) Cleavage of poly(A)-binding protein by poliovirus 3C proteinase inhibits viral internal ribosome entry site-mediated translation. J Virol 82:9389–9399

Brown CE, Sachs AB (1998) Poly(A) tail length control in Saccharomyces cerevisiae occurs by message-specific deadenylation. Mol Cell Biol 18:6548–6559

Cai X, Yang Y, Xia W, Kong H, Wang M, Fu W, Long M, Hu Y, Xu D (2018) RIP2 promotes glioma cell growth by regulating TRAF3 and activating the NFkappaB and p38 signaling pathways. Oncol Rep 39:2915–2923

Cavallari JF, Fullerton MD, Duggan BM, Foley KP, Denou E, Smith BK, Desjardins EM, Henriksbo BD, Kim KJ, Tuinema BR, Stearns JC, Prescott D, Rosenstiel P, Coombes BK, Steinberg GR, Schertzer JD (2017) Muramyl dipeptide-based postbiotics mitigate obesity-induced insulin resistance via IRF4. Cell Metab 25:1063–1074.e1063

Christofori G, Keller W (1988) 3′ cleavage and polyadenylation of mRNA precursors in vitro requires a poly(A) polymerase, a cleavage factor, and a snRNP. Cell 54:875–889

Copeland AM, Altamura LA, Van Deusen NM, Schmaljohn CS (2013) Nuclear relocalization of polyadenylate binding protein during rift valley fever virus infection involves expression of the NSs gene. J Virol 87:11659–11669

Copsey AC, Cooper S, Parker R, Lineham E, Lapworth C, Jallad D, Sweet S, Morley SJ (2017) The helicase, DDX3X, interacts with poly(A)-binding protein 1 (PABP1) and caprin-1 at the leading edge of migrating fibroblasts and is required for efficient cell spreading. Biochem J 474:3109–3120

Dominguez-Martinez DA, Nunez-Avellaneda D, Castanon-Sanchez CA, Salazar MI (2018) NOD2: activation during bacterial and viral infections, polymorphisms and potential as therapeutic target. Rev Invest Clin 70:18–28

Du Y, Bi J, Liu J, Liu X, Wu X, Jiang P, Yoo D, Zhang Y, Wu J, Wan R, Zhao X, Guo L, Sun W, Cong X, Chen L, Wang J (2014) 3Cpro of foot-and-mouth disease virus antagonizes the interferon signaling pathway by blocking STAT1/STAT2 nuclear translocation. J Virol 88:4908–4920

Egarnes B, Gosselin J (2018) Contribution of regulatory T cells in nucleotide-binding oligomerization domain 2 response to influenza virus infection. Front Immunol 9:132

Eliseeva IA, Lyabin DN, Ovchinnikov LP (2013) Poly(A)-binding proteins: structure, domain organization, and activity regulation. Biochem Mosc 78:1377–1391

Fan X, Han S, Yan D, Gao Y (2017) Foot-and-mouth disease virus infection suppresses autophagy and NF-small ka, CyrillicB antiviral responses via degradation of ATG5-ATG12 by 3C(pro). Cell Death Dis 8:e2561

Feng HH, Zhu ZX, Cao WJ, Yang F, Zhang XL, Du XL, Zhang KS, Liu XT, Zheng HX (2018) Foot-and-mouth disease virus induces lysosomal degradation of NME1 to impair p53-regulated interferon-inducible antiviral genes expression. Cell Death Dis 9:885

Gladue DP, O'Donnell V, Baker-Branstetter R, Holinka LG, Pacheco JM, Fernandez-Sainz I, Lu Z, Brocchi E, Baxt B, Piccone ME, Rodriguez L, Borca MV (2012) Foot-and-mouth disease virus nonstructural protein 2C interacts with Beclin1, modulating virus replication. J Virol 86:12080–12090

Gladue DP, O'Donnell V, Baker-Branstetter R, Holinka LG, Pacheco JM, Fernandez Sainz I, Lu Z, Ambroggio X, Rodriguez L, Borca MV (2013) Foot-and-mouth disease virus modulates cellular vimentin for virus survival. J Virol 87:6794–6803

Grubman MJ, Baxt B (2004) Foot-and-mouth disease. Clin Microbiol Rev 17:465–493

Huang B, Hu P, Hu A, Li Y, Shi W, Huang J, Jiang Q, Xu S, Li L, Wu Q (2019) Naringenin attenuates carotid restenosis in rats after balloon injury through its anti-inflammation and anti-oxidative effects via the RIP1-RIP3-MLKL signaling pathway. Eur J Pharmacol 855:167–174

Jing H, Fang L, Wang D, Ding Z, Luo R, Chen H, Xiao S (2014) Porcine reproductive and respiratory syndrome virus infection activates NOD2-RIP2 signal pathway in MARC-145 cells. Virology 458–459:162–171

Joachims M, Van Breugel PC, Lloyd RE (1999) Cleavage of poly(A)-binding protein by enterovirus proteases concurrent with inhibition of translation in vitro. J Virol 73:718–727

Kanda T, Ozawa M, Tsukiyama-Kohara K (2016) IRES-mediated translation of foot-and-mouth disease virus (FMDV) in cultured cells derived from FMDV-susceptible and -insusceptible animals. BMC Vet Res 12:66

Kanneganti TD, Lamkanfi M, Nunez G (2007) Intracellular NOD-like receptors in host defense and disease. Immunity 27:549–559

Kapoor A, Forman M, Arav-Boger R (2014) Activation of nucleotide oligomerization domain 2 (NOD2) by human cytomegalovirus initiates innate immune responses and restricts virus replication. PLoS ONE 9:e92704

Kobayashi M, Arias C, Garabedian A, Palmenberg AC, Mohr I (2012) Site-specific cleavage of the host poly(A) binding protein by the encephalomyocarditis virus 3C proteinase stimulates viral replication. J Virol 86:10686–10694

Kopparam J, Chiffelle J, Angelino P, Piersigilli A, Zangger N, Delorenzi M, Meylan E (2017) RIP4 inhibits STAT3 signaling to sustain lung adenocarcinoma differentiation. Cell Death Differ 24:1761–1771

Kuyumcu-Martinez NM, Joachims M, Lloyd RE (2002) Efficient cleavage of ribosome-associated poly(A)-binding protein by enterovirus 3C protease. J Virol 76:2062–2074

Kuyumcu-Martinez M, Belliot G, Sosnovtsev SV, Chang KO, Green KY, Lloyd RE (2004) Calicivirus 3C-like proteinase inhibits cellular translation by cleavage of poly(A)-binding protein. J Virol 78:8172–8182

Kuyumcu-Martinez NM, Van Eden ME, Younan P, Lloyd RE (2004) Cleavage of poly(A)-binding protein by poliovirus 3C protease inhibits host cell translation: a novel mechanism for host translation shutoff. Mol Cell Biol 24:1779–1790

Lee KH, Biswas A, Liu YJ, Kobayashi KS (2012) Proteasomal degradation of Nod2 protein mediates tolerance to bacterial cell wall components. J Biol Chem 287:39800–39811

Li D, Lei C, Xu Z, Yang F, Liu H, Zhu Z, Li S, Liu X, Shu H, Zheng H (2016) Foot-and-mouth disease virus non-structural protein 3A inhibits the interferon-beta signaling pathway. Sci Rep 6:21888

Li D, Yang W, Yang F, Liu H, Zhu Z, Lian K, Lei C, Li S, Liu X, Zheng H, Shu H (2016) The VP3 structural protein of foot-and-mouth disease virus inhibits the IFN-beta signaling pathway. FASEB J 30:1757–1766

Li C, Zhu Z, Du X, Cao W, Yang F, Zhang X, Feng H, Li D, Zhang K, Liu X, Zheng H (2017) Foot-and-mouth disease virus induces lysosomal degradation of host protein kinase PKR by 3C proteinase to facilitate virus replication. Virology 509:222–231

Li Z, Ning S, Su X, Liu X, Wang H, Liu Y, Zheng W, Zheng B, Yu XF, Zhang W (2018) Enterovirus 71 antagonizes the inhibition of the host intrinsic antiviral factor A3G. Nucl Acids Res 46:11514–11527

Li L, Fan H, Song Z, Liu X, Bai J, Jiang P (2019) Encephalomyocarditis virus 2C protein antagonizes interferon-beta signaling pathway through interaction with MDA5. Antivir Res 161:70–84

Liu H, Xue Q, Cao W, Yang F, Ma L, Liu W, Zhang K, Liu X, Zhu Z, Zheng H (2018) Foot-and-mouth disease virus nonstructural protein 2B interacts with cyclophilin A, modulating virus replication. FASEB J 32:6706–6723

Liu YL, Yan J, Zheng J, Tian QB (2018) (938)RHRK(941) is responsible for Ubiquitin specific protease 48 nuclear translocation which can stabilize NF-kappaB (p65) in the nucleus. Gene 669:77–81

Liu H, Zhu Z, Xue Q, Yang F, Cao W, Zhang K, Liu X, Zheng H (2019) Foot-and-mouth disease virus antagonizes NOD2-mediated antiviral effects by inhibiting NOD2 protein expression. J Virol 93:e00124–19

Moffat K, Howell G, Knox C, Belsham GJ, Monaghan P, Ryan MD, Wileman T (2005) Effects of foot-and-mouth disease virus nonstructural proteins on the structure and function of the early secretory pathway: 2BC but not 3A blocks endoplasmic reticulum-to-Golgi transport. J Virol 79:4382–4395

Moffat K, Knox C, Howell G, Clark SJ, Yang H, Belsham GJ, Ryan M, Wileman T (2007) Inhibition of the secretory pathway by foot-and-mouth disease virus 2BC protein is reproduced by coexpression of 2B with 2C, and the site of inhibition is determined by the subcellular location of 2C. J Virol 81:1129–1139

Moraes MP, Segundo FD, Dias CC, Pena L, Grubman MJ (2011) Increased efficacy of an adenovirus-vectored foot-and-mouth disease capsid subunit vaccine expressing nonstructural protein 2B is associated with a specific T cell response. Vaccine 29:9431–9440

Nembrini C, Kisielow J, Shamshiev AT, Tortola L, Coyle AJ, Kopf M, Marsland BJ (2009) The kinase activity of Rip2 determines its stability and consequently Nod1- and Nod2-mediated immune responses. J Biol Chem 284:19183–19188

Nystrom N, Berg T, Lundin E, Skog O, Hansson I, Frisk G, Juko-Pecirep I, Nilsson M, Gyllensten U, Finkel Y, Fuxe J, Wanders A (2013) Human enterovirus species B in ileocecal Crohn's disease. Clin Transl Gastroenterol 4:e38

Ren Y, Liu SF, Nie L, Cai SY, Chen J (2018) Involvement of ayu NOD2 in NF-kappaB and MAPK signaling pathways: insights into functional conservation of NOD2 in antibacterial innate immunit. Zool Res 40:77–88

Rodriguez Pulido M, Serrano P, Saiz M, Martinez-Salas E (2007) Foot-and-mouth disease virus infection induces proteolytic cleavage of PTB, eIF3a, b, and PABP RNA-binding proteins. Virology 364:466–474

Sabbah A, Chang TH, Harnack R, Frohlich V, Tominaga K, Dube PH, Xiang Y, Bose S (2009) Activation of innate immune antiviral responses by Nod2. Nat Immunol 10:1073–1080

Sachs AB, Davis RW (1989) The poly(A) binding protein is required for poly(A) shortening and 60S ribosomal subunit-dependent translation initiation. Cell 58:857–867

Sachs A, Davis R (1990) The poly(A)-binding protein is required for translation initiation and poly(A) tail shortening. Mol Biol Rep 14:73

Schmittgen TD, Livak KJ (2008) Analyzing real-time PCR data by the comparative C(T) method. Nat Protoc 3:1101–1108

Shaw MH, Reimer T, Kim YG, Nunez G (2008) NOD-like receptors (NLRs): bona fide intracellular microbial sensors. Curr Opin Immunol 20:377–382

Smith RWP, Anderson RC, Larralde O, Smith JWS, Gorgoni B, Richardson WA, Malik P, Graham SV, Gray NK (2017) Viral and cellular mRNA-specific activators harness PABP and eIF4G to promote translation initiation downstream of cap binding. Proc Natl Acad Sci U S A 114:6310–6315

Sun D, Wang M, Wen X, Cheng A, Jia R, Sun K, Yang Q, Wu Y, Zhu D, Chen S, Liu M, Zhao X, Chen X (2017) Cleavage of poly(A)-binding protein by duck hepatitis A virus 3C protease. Sci Rep 7:16261

Sweeney TR, Cisnetto V, Bose D, Bailey M, Wilson JR, Zhang X, Belsham GJ, Curry S (2010) Foot-and-mouth disease virus 2C is a hexameric AAA+protein with a coordinated ATP hydrolysis mechanism. J Biol Chem 285:24347–24359

Tian J, Liu Y, Liu X, Sun X, Zhang J, Qu L (2018) Feline herpesvirus 1 (FHV-1) US3 blocks type I IFN signal pathway by targeting IRF3 dimerization in a kinase-independent manner. J Virol 92: e00047–18

Vassalli JD, Huarte J, Belin D, Gubler P, Vassalli A, O'Connell ML, Parton LA, Rickles RJ, Strickland S (1989) Regulated polyadenylation controls mRNA translation during meiotic maturation of mouse oocytes. Genes Dev 3:2163–2171

Vissers M, Remijn T, Oosting M, de Jong DJ, Diavatopoulos DA, Hermans PW, Ferwerda G (2012) Respiratory syncytial virus infection augments NOD2 signaling in an IFN-beta-dependent manner in human primary cells. Eur J Immunol 42:2727–2735

Wang D, Fang L, Li P, Sun L, Fan J, Zhang Q, Luo R, Liu X, Li K, Chen H, Chen Z, Xiao S (2011) The leader proteinase of foot-and-mouth disease virus negatively regulates the type I interferon pathway by acting as a viral deubiquitinase. J Virol 85:3758–3766

Wang D, Fang L, Li K, Zhong H, Fan J, Ouyang C, Zhang H, Duan E, Luo R, Zhang Z, Liu X, Chen H, Xiao S (2012) Foot-and-mouth disease virus 3C protease cleaves NEMO to impair innate immune signaling. J Virol 86:9311–9322

Wang J, Wang Y, Liu J, Ding L, Zhang Q, Li X, Cao H, Tang J, Zheng SJ (2012) A critical role of N-myc and STAT interactor (Nmi) in foot-and-mouth disease virus (FMDV) 2C-induced apoptosis. Virus Res 170:59–65

Wormington M, Searfoss AM, Hurney CA (1996) Overexpression of poly(A) binding protein prevents maturation-specific deadenylation and translational inactivation in Xenopus oocytes. EMBO J 15:900–909

Wu XM, Chen WQ, Hu YW, Cao L, Nie P, Chang MX (2018) RIP2 is a critical regulator for NLRs signaling and MHC antigen presentation but not for MAPK and PI3K/Akt pathways. Front Immunol 9:726

Xue Q, Liu H, Zhu Z, Yang F, Xue Q, Cai X, Liu X, Zheng H (2018) Seneca Valley virus 3C protease negatively regulates the type I interferon pathway by acting as a viral deubiquitinase. Antivir Res 160:183–189

Zheng H, Guo J, Jin Y, Yang F, He J, Lv L, Zhang K, Wu Q, Liu X, Cai X (2013) Engineering foot-and-mouth disease viruses with improved growth properties for vaccine development. PLoS ONE 8:e55228

Zheng W, Li X, Wang J, Li X, Cao H, Wang Y, Zeng Q, Zheng SJ (2014) A critical role of interferon-induced protein IFP35 in the type I interferon response in cells induced by foot-and-mouth disease virus (FMDV) protein 2C. Arch Virol 159:2925–2935

Zheng Y, Shang F, An L, Zhao H, Liu X (2018) NOD2-RIP2 contributes to the inflammatory responses of mice in vivo to Streptococcus pneumoniae. Neurosci Lett 671:43–49

Zhu B (2018) Haemophilus parasuis infection activates NOD1/2-RIP2 signaling pathways in PK-15 cells. Dev Comp Immunol 79:158–165

Zhu Z, Shi Z, Yan W, Wei J, Shao D, Deng X, Wang S, Li B, Tong G, Ma Z (2013) Nonstructural protein 1 of influenza A virus interacts with human guany late-binding protein 1 to antagonize antiviral activity. PLoS ONE 8:e55920

Zhu Z, Wang G, Yang F, Cao W, Mao R, Du X, Zhang X, Li C, Li D, Zhang K, Shu H, Liu X, Zheng H (2016) Foot-and-mouth disease virus viroporin 2B antagonizes RIG-I-mediated antiviral effects by inhibition of its protein expression. J Virol 90:11106–11121

Zhu Z, Li C, Du X, Wang G, Cao W, Yang F, Feng H, Zhang X, Shi Z, Liu H, Tian H, Li D, Zhang K, Liu X, Zheng H (2017) Foot-and-mouth disease virus infection inhibits LGP2 protein expression to exaggerate inflammatory response and promote viral replication. Cell Death Dis 8:e2747